

# Resin-to-Resin Circularity in Chemical Recycling of Dicyclopentadiene-Based Cycloolefin Resins

Zhen Xu, Mason L. Witko, Hongqian Zheng, Julia Im, Shira Haber, Ankita Ghosh, Maxwell C. Venetos, Jeffrey A. Reimer, Kristin A. Persson, and Brett A. Helms\*



Cite This: *J. Am. Chem. Soc.* 2025, 147, 25613–25621



Read Online

ACCESS |



Metrics & More

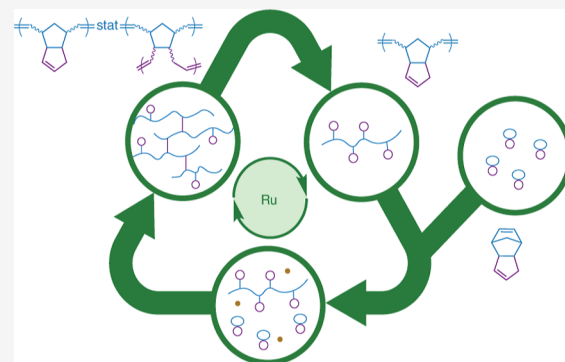


Article Recommendations



Supporting Information

**ABSTRACT:** Cycloolefin resins (CORs) comprising dicyclopentadiene (DCPD) cross-linkers are high performance thermosets for diverse single-use applications. If it were possible to carry out deconstruction of DCPD thermosets through exclusive reformation of the cyclopentene ring in DCPD, then linear polyDCPD chains could re-enter subsequent manufacturing cycles and enable resin-to-resin circularity. Here, we develop a chemical recycling process whereby linear polyDCPD recyclates are generated from end-of-life commercial and model CORs, including copolymers, using a second-generation Hoveyda–Grubbs ruthenium(II) alkylidene catalyst for deconstruction via ring-closing metathesis. The properties of first-generation DCPD thermosets were reproduced across subsequent generations of recycling and reuse, where up to 84% of linear DCPD was retrievable from end-of-life thermosets after deconstruction. We further quantify how comonomer incorporation, the curing process, and aging affect round-trip material efficiency and the quality of regenerated thermosets.



## INTRODUCTION

Cycloolefin resins (CORs) comprising dicyclopentadiene (DCPD) cross-linkers are widely used high-performance thermosets.<sup>1–6</sup> Cycloolefin monomers and cross-linkers incorporated alongside DCPD provide access to tunable material properties.<sup>7–11</sup> There has been growing interest in deploying DCPD resins in additive manufacturing using energy-efficient thermal or photochemical processes (Figure 1a).<sup>1,12–15</sup> Yet, end-of-life management of DCPD resin waste presents an ongoing challenge due to low recyclate yields upon network deconstruction. This challenge has thus far hindered progress in achieving cross-linker-to-cross-linker (i.e., DCPD-to-DCPD) circularity through chemical recycling.<sup>16</sup>

As a counterpoint and potential endgame, here we demonstrate resin-to-resin circularity in DCPD-based CORs by developing a process whereby a second-generation Hoveyda–Grubbs ruthenium(II) alkylidene catalyst promotes deconstruction via ring-closing metathesis (RCM), producing soluble reusable linear polyDCPD recyclates upon reformation of cyclopentene (CP) rings along the chain (Figure 1c). By tailoring the temperature and solvent-to-resin ratio during thermoset deconstruction, we define parameters for obtaining linear pDCPD recyclates with structural uniformity in isolated yields up to 84%. Despite changes in DCPD thermosets upon extensive oxidation aging and thermal curing, linear pDCPD recyclates with essentially the same molecular characteristics and negligible contamination were obtained in comparable

yields. We were able to reproduce the thermomechanical properties of first-generation (i.e., pristine) DCPD thermosets across several generations of chemical recycling and reuse by blending linear pDCPD recyclates with pristine liquid resin, establishing strong foundations for resin-to-resin circularity. To broaden the scope, we studied the impact of comonomer reactivity relative to the norbornene moieties in DCPD on the recyclability. We found that monomers polymerizing at similar rates to DCPD afforded more homogeneous recyclates, capable of reproducing first-generation material properties faithfully in subsequent material generations.

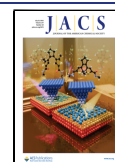
RCM depolymerization of DCPD thermosets complements the body of work on the deconstruction of cycloolefin polymers and leverages both fundamental and practical understanding of ring-strain energy (RSE) in cycloolefin monomers. For example, while the RSE of cyclohexene is too low to polymerize, it is possible to create “polycyclohexene” by copolymerizing a diene and an alkene; this allows for RCM depolymerization of linear polymers.<sup>17</sup> Similarly, 4-cycloheptenone’s moderate RSE can be leveraged for rapid

Received: April 18, 2025

Revised: June 26, 2025

Accepted: June 27, 2025

Published: July 14, 2025



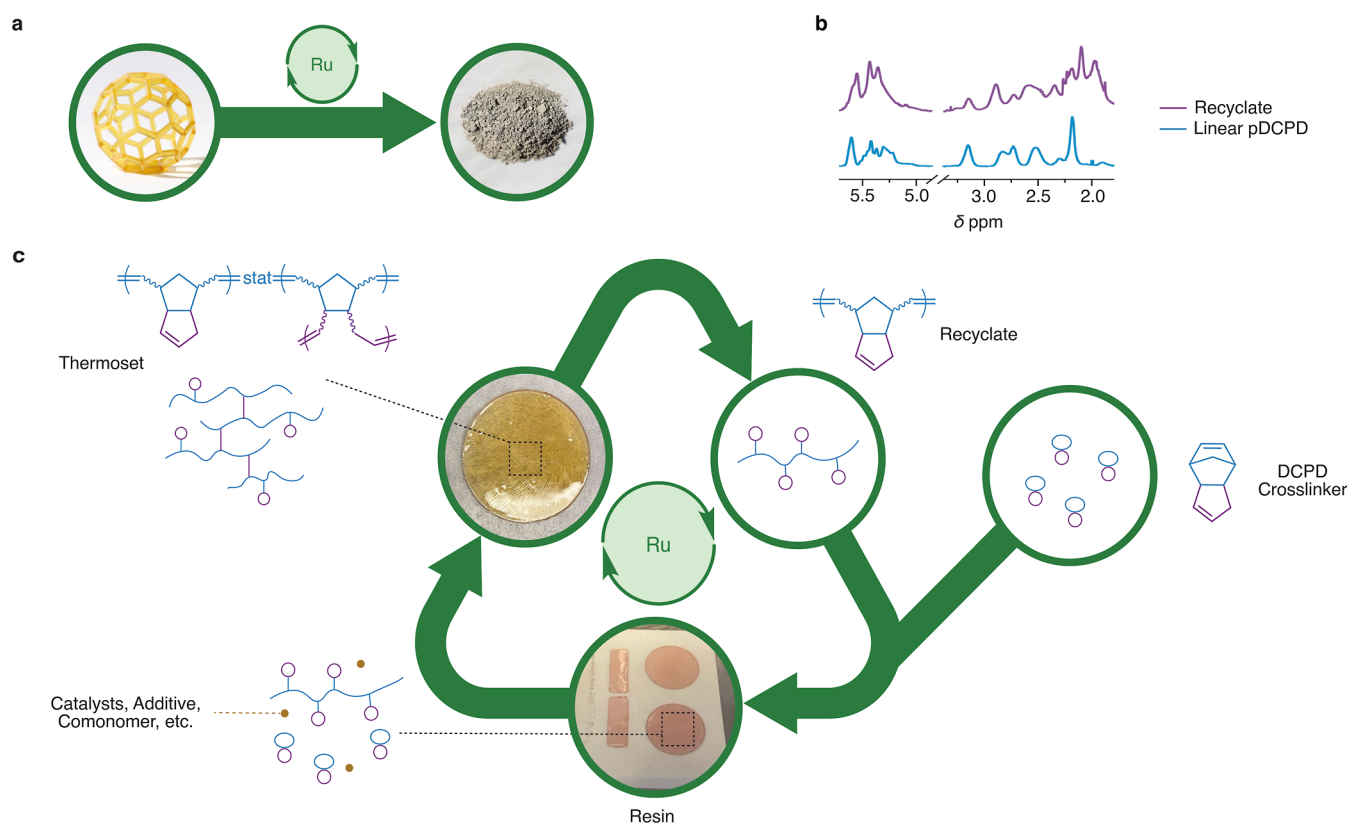


**Figure 1.** (a) Deconstruction of a commercial 3-D printed cycloolefin resin-based fullerene (polySpectra) into a polymeric recyclate through the action of a ring-closing metathesis depolymerization catalyst. (b) <sup>1</sup>H NMR spectrum of the polymeric cycloolefin resin recyclate alongside that for an authentic sample of linear polydicyclopentadiene (polyDCPD). (c) Schematic of the envisioned and realized resin-to-resin circularity, leveraging the chemistry of DCPD.

polymerization and then functionalized to lower RSE to enable RCM depolymerization.<sup>18</sup> High concentration RCM depolymerization can also be carried out to cyclic macromonomers, avoiding cumulative energy and mass losses inherent to RCM depolymerization to small-molecule ring monomers.<sup>19</sup> Yet, here, DCPD features a highly strained norbornene moiety that enables rapid polymerization; it remains difficult to reform via control over the underlying ring–chain equilibrium. Thus, our work challenges the conventional wisdom that copolymerization of DCPD with specialty monomers featuring cleavable functionality is needed for thermoset deconstruction.<sup>15,20–27</sup> Thermal reprocessing of DCPD thermosets has also been reported and leverages the reactivity of ruthenium(II) alkylidene catalysts left behind after curing to promote metathesis bond exchange after end-of-life.<sup>7</sup> This alternative places constraints on materials processing and handling since thermal reprocessing relies on the retention of catalyst activity and low steric hindrances for comonomers. Our emphasis here on resin-to-resin circularity relaxes the aforementioned constraints on monomers, cross-linkers, and catalysts,<sup>28–35</sup> setting the stage for transformative advancements in the sustainable management of commercial thermosets cross-linked with DCPD.

## RESULTS AND DISCUSSION

DCPD features two distinct polymerizable cycloolefins: the first is a high-ring strain cycloolefin for fast propagation of linear segments; the second is a low-ring strain cycloolefin for cross-linking. Whereas the linear segments are challenging to depolymerize, the deconstruction of DCPD thermosets

nevertheless may proceed through selective reformation of the low-ring strain CP ring via ruthenium-catalyzed RCM. If successful, linear polyDCPD chains could re-enter subsequent manufacturing cycles as a versatile recyclate that enables resin-to-resin circularity (Figure 1c).

DCPD polymerizes initially by ring-opening metathesis polymerization of the strained norbornene, and the resulting chains are subsequently cross-linked into a network through ring-opening of pendant CPs. Approximately 5–15% of pendant CP moieties participate in cross-linking.<sup>15,20</sup> Olefin addition further contributes to cross-linking density for resins baked at elevated temperature (120–185 °C) after curing, which enhances their thermomechanical properties. Deconstruction of commercial CORs with RCM depolymerization second-generation Hoveyda–Grubbs catalyst (HG2) (2 mol %) results in low yields (12–26%) of a previously unidentified, yet soluble recyclate (Figure 1a). We determined that this recyclate was polymeric with  $M_n = 2510$ ,  $M_w = 3250$ , and  $\bar{D} = 1.30$ . We also noted that its <sup>1</sup>H NMR spectrum bore a striking resemblance to linear polyDCPD (Figures 1b and S1 and S2), though it still possessed a number of overlapping peaks between 2.5 and 0.5 ppm not attributable to linear pDCPD. From the DOSY NMR spectra for recyclates baked at different temperatures postcure, we confirmed that these additional <sup>1</sup>H NMR peaks likely stem from comonomer incorporation in commercial resin formulations, since they have the same diffusion coefficients (Figures S3–S5). These insights suggested to us that it should be possible to carry out deconstruction of DCPD thermosets using a RCM catalyst if they generate soluble linear polyDCPD chains that re-enter

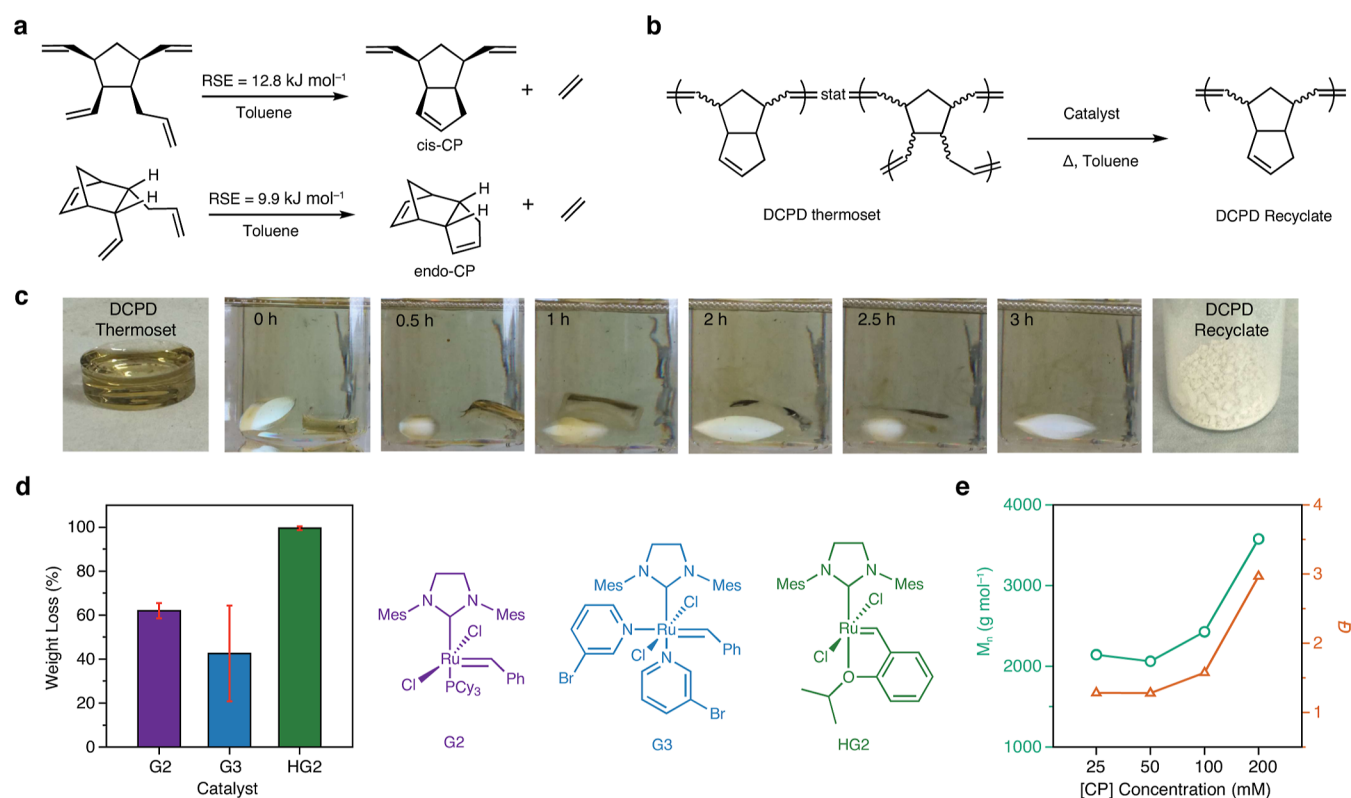


**Figure 2.** DCPD thermoset deconstruction via ring-closing metathesis. (a) Ring-strain energies (RSEs) calculated for cyclopentene rings in DCPD derivatives. (b) Chemical structures of DCPD thermoset deconstruction. (c) DCPD in its initial state as a cross-linked thermoset, its deconstruction trajectory from suspended to dissolved solid over time, and final appearance after filtering out unwanted solids and then precipitating and drying the reusable DCPD recyclate. (d) Weight loss (%) using G2, G3, and HG2 after carrying out thermoset deconstruction over 3 h. (e) Number-average molar masses ( $M_n$ ) and dispersities ( $\bar{D}$ ) of DCPD recyclates as a function of [CP] concentration during DCPD thermoset deconstruction.

subsequent manufacturing cycles to enable resin-to-resin circularity.

As an initial test of our hypothesis, we calculated the ethenolysis RSEs for representative CP moieties in endo- (Figure 2a) and exo-DCPD (Figure S6). We did so using the enthalpy changes of the RCM reactions that produce the target DCPD derivatives and ethene molecules. We considered contributions from different conformers for both cycloolefins and their acyclic diene counterparts, using the Conformer–Rotamer Ensemble Sampling Tool (CREST) algorithm.<sup>36</sup> We took into account the effects of solvent with the SMD implicit solvent model to simulate cross-linking in decalin as well as deconstruction in toluene.<sup>37</sup> We compared these values with those of a well-known circular cycloolefin: CP, which serves as a reference. Fused CP functionalities in DCPD exhibited low RSE values of 12.8 and 9.9 kJ mol<sup>-1</sup> in toluene before (endo-CP) and after (cis-CP) norbornene moieties are ring-opened, respectively (Figure 2a). For comparison, RSE for CP in toluene is 25.1 kJ mol<sup>-1</sup>, indicating depolymerization of CP in cross-linked DCPD is feasible. Notably, CP rings also exhibited low RSE values of 13.4 (endo-CP) and 10.2 kJ mol<sup>-1</sup> (cis-CP) in decalin, consistent with the low conversion (5–15%) of CP rings during DCPD curing and other functionalized CP monomers.<sup>38</sup> CP's RSE predominantly stems from torsional effects,<sup>39</sup> so it seems logical that CP rings within DCPD would have lower RSE given its reduction in eclipsing bonds.

Having established the potential for depolymerizability of CP rings in DCPD in our computational studies, we sought out to verify the prediction in cured DCPD resins, which we

prepared from DCPD at 120 °C for 60 min in the presence of 0.04 mol % Grubbs second-generation catalyst (G2).<sup>20</sup> We carried out this curing step under an inert nitrogen atmosphere to prevent any unwanted reactions, e.g., oxidative cross-linking or olefin-to-olefin addition. It is worth noting that DCPD is a solid at ambient temperature; accordingly, we incorporated 5 wt % ethylidene norbornene (ENB) to suppress the melting point. We refer to this mixture as DCPD resin throughout the manuscript. The mechanical properties of these DCPD thermosets were comparable to previous reports, including tensile strength, which remained similar to pristine DCPD at various recyclate weight percents (Table S1).<sup>12,21</sup>

To showcase their deconstruction, we treated the thermosets at high dilution ([CP] = 50 mM) with 0.2 mol % HG2 in toluene. The polymer networks underwent swelling in toluene within 1 h, producing a nearly transparent, colorless gel (Figure 2c). After 3 h, deconstruction of the network was complete. After precipitation from cold methanol, we recovered a nearly colorless solid in 84% yield. We characterized these solids using nuclear magnetic resonance spectroscopy (NMR), size-exclusion chromatography (SEC), and matrix-assisted laser desorption/ionization time-of-flight mass spectrometry (MALDI-ToF). Detailed molecular characteristics of recyclates are summarized (Table S2). Most notably, the <sup>1</sup>H and <sup>13</sup>C NMR spectra resembled those of linear non-cross-linked pDCPD samples. More careful analysis by <sup>13</sup>C NMR of the recyclate solution revealed that the percentage of ring-opened CP in the recyclate was in the range of 0–1.5% (Figures S10–S15). By SEC, the recovered solids had a number-average



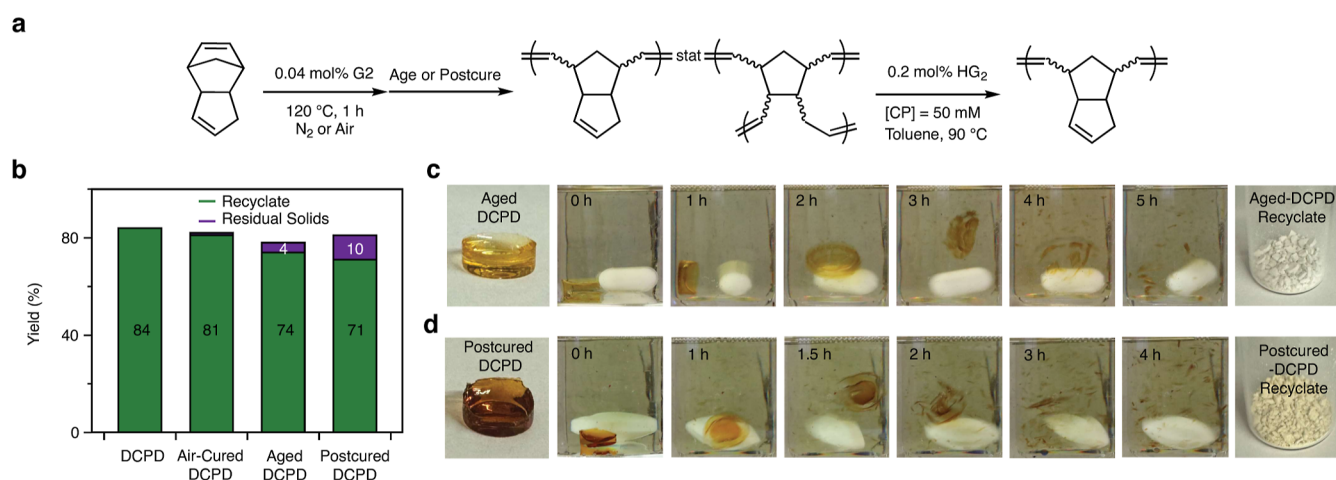


**Figure 3.** Curing and aging effects on the resin-to-resin recyclability of DCPD thermosets. (a) Chemical structures of DCPD curing and thermoset deconstruction under various conditions. (b) Recovery yield of DCPD recyclate and residual solids under various curing and aging conditions. (c) Visual progression of the deconstruction trajectory of aged DCPD thermoset over time. (d) Visual progression of the deconstruction trajectory of postcured DCPD thermoset over time.

molar mass ( $M_n$ ) of  $2100 \text{ g mol}^{-1}$  and a dispersity ( $\bar{D}$ ) of 1.28. Based on these data, we estimated that there was one ring-opened CP for every 7–15 DCPD repeating units during DCPD curing. Thus, CP conversion is estimated to be 6–15%, in line with previous reports.<sup>15,20</sup> Factors contributing to the successes or failures of DCPD thermoset deconstruction are discussed thoroughly below. Furthermore, MALDI-ToF revealed that the recyclates exhibited a peak at  $1033.6 \text{ m/z}$ , which contains an ethyl vinyl ether chain end and 6 repeating units of DCPD (Figure S9). Specifically, in coming to the procedure above, we screened process parameters for affecting thermoset deconstruction, focusing on catalyst and polymer concentration. We considered the implications of catalyst–polymer interactions as well as ring–chain equilibria on the deconstruction yield and recyclate quality. With regard to catalyst choice for thermoset deconstruction, it is important that ligands at the metal center promote ring-closing over ring-opening.<sup>40</sup> Additionally, the Jacobsen–Stockmayer theory indicates that for ring monomers to form, in this case reformation of CP pendants, RCM should be carried out at a sufficiently high dilution.<sup>41</sup>

Regarding the catalyst selection, we carried out the reactions in toluene ( $[\text{CP}] = 50 \text{ mM}$ ) at  $90^\circ\text{C}$  in the presence of 0.2 mol % G2, G3, or HG2 for 3 h (Figure 2d). Remarkably, deconstruction using HG2 led to near-complete dissolution of the DCPD thermosets (99.5%). By comparison, the extents of deconstruction with G2 and G3, as calculated by the percentage of weight loss, were only 62% and 43%, respectively. Thus, HG2 is a substantially more effective RCM catalyst for DCPD deconstruction. This may be explained by the “boomerang mechanism”, for which ample evidence has been recently produced.<sup>42</sup> This mechanism involves a release–return pathway in which isopropoxystyrene disassociates from the catalyst’s ruthenium center, increasing catalyst reactivity by creating space for the approach of reactants. After the catalyst facilitates reactions, isopropoxystyrene may return to the catalyst, increasing its lifetime. Yet, it remained unclear how sensitive to concentration might DCPD deconstruction be in the presence of HG2.

Regarding dilution and ring–chain equilibria, we conducted the deconstruction at different ratios of solids to solvent,

analyzing the characteristics of the soluble products by SEC (Figures 2e and S16). It is worth noting DCPD thermosets were completely deconstructed, regardless of the concentration used. However, as predicted, when carried out in high dilution ( $[\text{CP}] = 25$  and  $50 \text{ mM}$ ), deconstruction produced recyclates with number-average molar masses ( $M_n$ ) of 2100 and  $2100 \text{ g mol}^{-1}$ , respectively; the dispersity ( $\bar{D}$ ) was 1.28 for both recyclates. MALDI-ToF analysis of the 50 mM recyclate found a  $M_n$  of  $1200 \text{ g mol}^{-1}$  (Figure S9), which is expected to be lower than the true  $M_n$  value of the sample, as lower molecular weight peaks typically have higher intensities. At higher concentrations favoring cross-links, e.g., 100 and 200 mM, deconstruction was incomplete, evidenced by a second peak at shorter retention times in the SEC traces. Quantitatively,  $M_n$  values of the recyclates increased from  $2400 \text{ g mol}^{-1}$  for 100 mM to  $3600 \text{ g mol}^{-1}$  for 200 mM, while  $\bar{D}$  values were 1.57 and 2.97, respectively.

Having established parameters for efficient DCPD thermoset deconstruction to linear polyDCPD recyclates, we sought to understand how different aging or curing conditions affected deconstruction outcomes (Figure 3). It has been shown that aging long-term as well as high-temperature processing postcuring leads to increases in cross-linking density via oxidative cross-linking and olefin-to-olefin addition, respectively.<sup>12,43,44</sup> First, we investigated how oxidative cross-linking affected thermoset recyclability. When we cured DCPD resins in air, instead of inert atmosphere, subsequent deconstruction at high dilution with HG2 left behind only a small amount ( $\sim 1 \text{ wt } \%$ ) of insoluble residual solids.<sup>15</sup> The linear polyDCPD recyclate yield dropped only slightly, from 84% to 81%. Further aging DCPD thermosets, e.g., at  $60^\circ\text{C}$  for 6 days, resulted in a further decrease in the linear polyDCPD recyclate yield to 74%. Oxidation and likely densification at the surface of the thermoset, tracked in time-lapsed photos (Figure 3c), resulted in a slower overall deconstruction from 3 to 5 h; however, once the solvent swelled the network and the catalyst gained access to reactive sites, deconstruction proceeded as it would have otherwise.

We retrieved the dense residual solids (4%) after deconstruction (Figure 3c) and characterized them by solid-state NMR and Fourier transform infrared spectroscopy (FT-

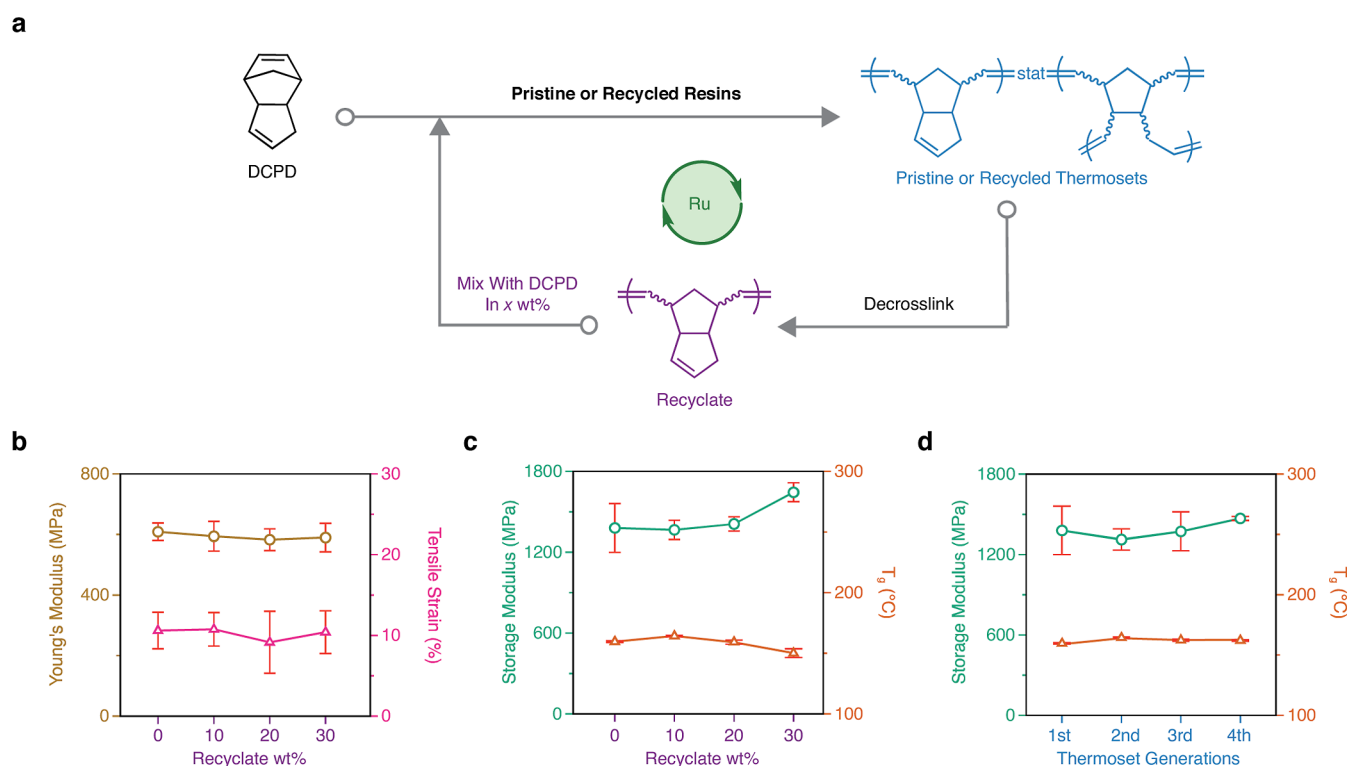


**Figure 4.** Resin-to-resin circularity enabled by incorporating solid DCPD recyclates into liquid DCPD resins. (a) Schematic illustration of resin-to-resin circularity from DCPD monomer resins, DCPD thermoset to linear polyDCPD recyclates. (b) Young's modulus and tensile strain measured by tensile tests as a function of recycle weight percentage in the second-generation of DCPD thermoset. (c) Storage moduli and glass transition temperatures ( $T_g$ ), as measured by DMA, as a function of recycle weight percentage in second-generation of DCPD thermosets. (d) Storage modulus and  $T_g$  measured by DMA as a function of DCPD thermoset generations.

IR) (Figures S17–S19). These recalcitrant solids exhibited characteristic O–H and C=O stretching in FT-IR and carbonyl signals in NMR. Oxidation rendered an outer portion of the thermoset insoluble during RCM deconstruction, suggesting cross-linking is concurrent with oxidation. There is literature precedent for the formation of a layer of oxidized material on pDCPD surfaces, as shown by FTIR analysis on pDCPD films.<sup>43</sup> In stark contrast, the recovered aged-DCPD recyclates did not show immediate signs of oxidation by FT-IR (Table S1 and Figure S17). In this way, we surmised that resin deconstruction with HG2 unexpectedly removes unwanted oxidized impurities that arise from aging long-term, returning structurally uniform recyclates that are indistinguishable from those retrieved from unaged samples.

Next, we sought to understand how thermal postcuring affected recyclability. Thermal postcuring typically invokes olefin-to-olefin addition to further enhance the thermomechanical properties of DCPD thermosets, here by increasing its glass transition temperature ( $T_g$ ) by 20 °C (Figure S20).<sup>12,44</sup> We deconstructed the postcured DCPD-C in 71% yield with 10% insoluble residual solids. Similarly, we achieved recyclates with similar characteristics (Figures S21–S23). It is worth noting that state-of-the-art analytical capabilities are not yet able to distinguish the characteristics of olefin-to-olefin addition from the other bonding motifs present; therefore, we were not able to precisely quantify the extent of olefin-to-olefin addition in the recyclates. Nonetheless, despite a confluence of changes in thermoset structure, composition, and properties that occur with aging or postcuring, deconstruction proceeded readily with only slight decreases in the yield of soluble linear DCPD recycle. While the

autoxidation affects yield, it is worth noting that the same process can be seen as desirable as it allows for excellent adhesion of paints and aids in bonding to coatings.<sup>4</sup> The small amount of insoluble residual solids was also found to confine impurities therein; these solids were easily separated from reusable linear DCPD recyclates by simple filtration.

To demonstrate resin-to-resin circularity, we blended linear polyDCPD recyclates with first-generation DCPD liquid resins for subsequent curing. To understand the extent to which we could incorporate the linear DCPD recyclates without compromising the thermoset properties, we conducted tensile tests and dynamic mechanical analysis (DMA) on a series of generations of DCPD thermosets. These tests measured mechanical properties as a function of recycle content in subsequent generations of recycled resins for comparison to first-generation thermosets (0 wt %) (Table S2 and Figures S24–S26). When we mixed recyclates up to 30 wt % with liquid resin, there were no significant changes in Young's moduli or tensile strains for second-generation thermosets (Figure 4b). However,  $T_g$ , which was determined by the  $\tan \delta$  peak in the DMA traces, decreased by approximately 10 °C in thermosets containing 30 wt % (Figure 4c). As well, the  $\tan \delta$  trace exhibited a shoulder peak around 160 °C, suggesting heterogeneity (Figure S24). We concluded that incorporating DCPD recyclates up to at least 20 wt % maintains the necessary microstructure and mechanical properties to reproduce the characteristics of first-generation materials. This is similar to the amount allowable when introducing mechanically recycled thermoplastics to pristine resin to maintain manufacturability and performance, which is noteworthy.<sup>45,46</sup>

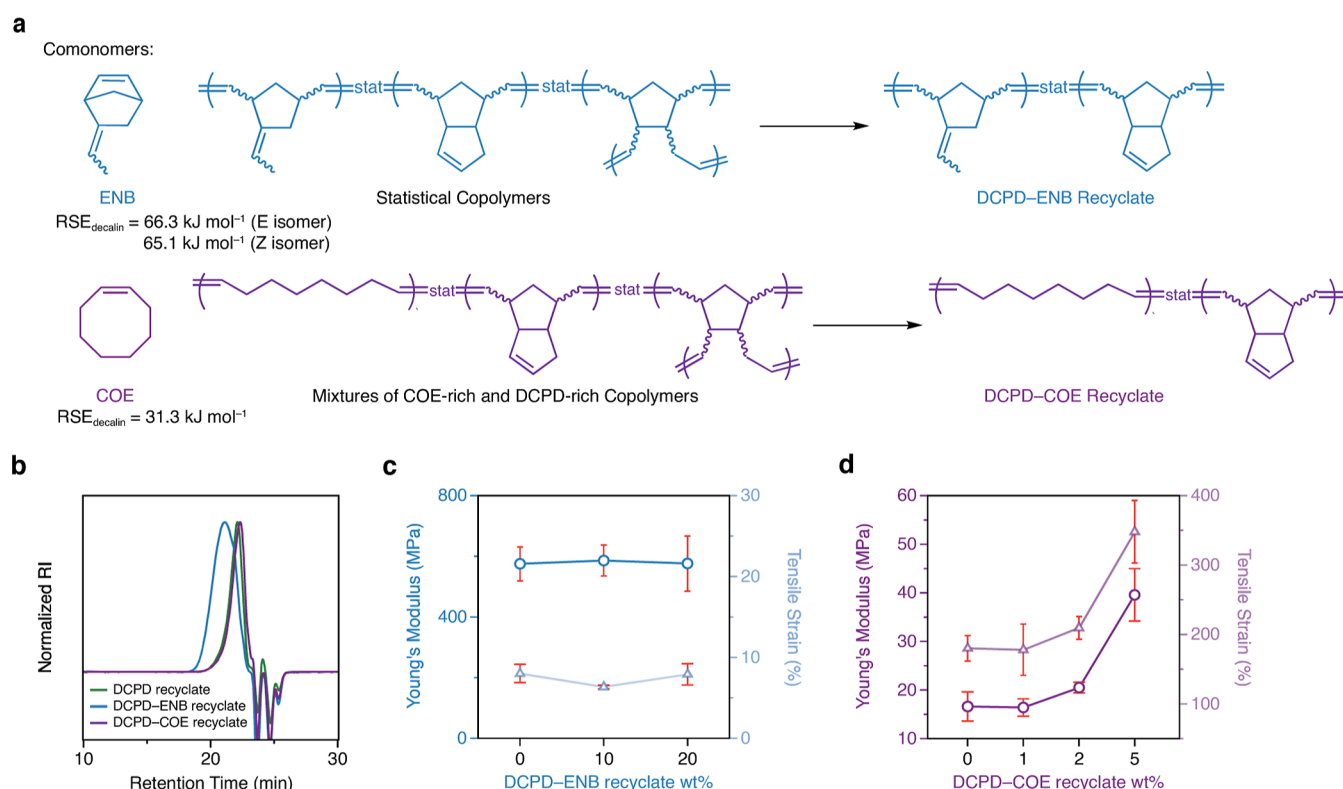


**Figure 5.** Resin-to-resin circularity in DCPD copolymers. (a) Chemical structures of comonomers, DCPD copolymer thermosets, and recyclates. (b) SEC traces of DCPD, DCPD-ENB, and DCPD-COE recyclates. (c) Young's modulus and tensile strain measured by tensile tests as a function of DCPD-ENB recyclate weight percentage in the second generation of DCPD-ENB thermoset. (d) Young's modulus and tensile strain measured by tensile tests as a function of DCPD-COE recyclate weight percentage in the second generation of DCPD-COE thermoset.

We further investigated the characteristics of recyclates and thermosets across subsequent manufacturing cycles using 10 wt % recyclate incorporation. Recyclate recovery yields remained unchanged after the second and third cycles of deconstruction, e.g., 79% and 78%, respectively, compared to 81% in DCPD thermosets cured under air. NMR and MALDI-ToF analyses of recyclates from the first to third generations were nearly identical (Figures S27–S29). We used DMA to evaluate the thermomechanical properties of recycled materials from first-, second-, third-, and fourth-generation thermosets (Figure S30). We did not observe substantial changes in the storage moduli or  $T_g$  (Figure 4d). These experiments demonstrated the feasibility of resin-to-resin circularity, whereby linear polyDCPD chains could re-enter subsequent manufacturing cycles and reproduce properties of first-generation DCPD thermosets across several generations of recycling and reuse.

To understand resin-to-resin circularity in DCPD copolymers with more broadly tunable mechanical properties, we synthesized copolymers by mixing DCPD with comonomers, including ENB or cyclooctene (COE) in 1:1 molar ratio. DCPD-ENB thermosets exhibited similar properties to DCPD thermosets, while DCPD-COE was elastomeric as expected.<sup>9,47</sup> We then investigated their deconstruction and regeneration behaviors. We selected these two comonomers due to their different RSE values in decaline: 66.3 kJ mol<sup>-1</sup> for the E isomer of ENB, 65.1 kJ mol<sup>-1</sup> for the Z isomer of ENB, and 31.3 kJ mol<sup>-1</sup> for the COE (Figure 5a). ENB, whose RSE values are comparable to the norbornene moiety of DCPD, is likely to form statistical copolymers during curing, while copolymerizing with COE will result in a mixture of COE-rich

and DCPD-rich copolymers.<sup>48</sup> We viewed these distinctions as likely to lead to changes in the characteristics and recyclability of the recyclates. Evidently, the DCPD-ENB recyclate exhibited an increase in  $M_n$  from 2060 to 3260 g mol<sup>-1</sup> (Figure 5b). On the other hand,  $M_n$  of the DCPD-COE recyclate remained largely unchanged compared to that of a DCPD recyclate. We also characterized these recyclates using NMR and MALDI-ToF along with accompanying DMA, DSC, and tensiometry data for pristine and recycled resins incorporating variable amounts of recyclate (Figures S31–S41).

These differences in composition and  $M_n$  also translated to variation in resin-to-resin recyclability (Table S3). Specifically, the DCPD-ENB recyclate could be incorporated into regenerated DCPD-ENB resins with similar properties as first-generation copolymer thermosets up to 20 wt %. This is similar to the observed effects of recyclate incorporation in DCPD samples (Figures S37–S39). The one noticeable difference is in tensile strength, which remains similar to pristine DCPD-ENB at 20 wt % recyclate incorporation but is lower at 10 wt % recyclate incorporation. Conversely, DCPD-COE recyclates, containing DCPD-rich and COE-rich fragments in their composition, led to a low incorporation weight percentage to maintain similar thermal and mechanical properties (Figures 5c, S40, and S41). Above 1 wt %, the Young's modulus and tensile strain of recycled materials increased dramatically from 16.6 MPa and 180% for pristine to 39.6 MPa and 380% for DCPD-COE containing 5 wt % recyclate (Figure 5d). Furthermore, tensile strength also increased greatly, from 1.98 MPa for pristine DCPD-COE to 3.32 MPa for 5 wt % recyclate DCPD-COE. This is contrasted with the somewhat similar tensile strengths of 1.59



and 1.90 MPa for 1 and 2 wt % recyclate, respectively. These experiments not only validated the applicability of resin-to-resin circularity in DCPD copolymers but also provided insight into how the reactivity of the monomer versus that of the cross-linker affected resin recyclability via RCM during deconstruction. For example, replacing cis-COE with trans-COE will likely improve recyclability due to the comparable ring strain between trans-COE and norbornene.<sup>49</sup>

## CONCLUSION

Our findings demonstrate that resin-to-resin circularity is capable of recycling high-performance thermosetting materials based on DCPD, which have been largely out of reach. By benchmarking theoretical predictions with experimental data, we validate our design concept and its practical implementation. We find that the careful selection of ruthenium(II) alkylidene catalyst and depolymerization concentration is vital for enabling DCPD deconstruction to well-defined reusable linear DCPD and DCPD-copolymer recyclates. We are able to achieve high yields of these recyclates while also showcasing their high quality. Furthermore, when industrially relevant postcuring processes are implemented and when accelerated aging has been undertaken to mimic changes across the use-phase of the thermoset, our catalyst-enabled deconstruction process produces reusable materials that are self-purified from impurities related to olefin-to-olefin addition and oxidation with only slight decreases in yield. Given the approach is applicable to DCPD copolymers with diverse tunable useful mechanical properties, we anticipate that resin-to-resin circularity will not only advance the future development of DCPD materials in a more sustainable manner but also inform the future design of cross-linkers to redefine the accessible chemical space for future cycloolefin thermoset circularity.

## ASSOCIATED CONTENT

### Supporting Information

The Supporting Information is available free of charge at <https://pubs.acs.org/doi/10.1021/jacs.5c06626>.

Additional experimental details, materials and methods, including NMR spectra of recyclate and linear pDCPD, calculated RSE values, MALDI-ToF, SEC, FT-IR, DMA, DSC, and tensile test analyses (PDF)

## AUTHOR INFORMATION

### Corresponding Author

**Brett A. Helms** — *Materials Sciences Division, Lawrence Berkeley National Laboratory, Berkeley 94720 California, United States; The Molecular Foundry, Lawrence Berkeley National Laboratory, Berkeley 94720 California, United States; Joint BioEnergy Institute, Emeryville 94608 California, United States*; [orcid.org/0000-0003-3925-4174](https://orcid.org/0000-0003-3925-4174); Email: [bahelms@lbl.gov](mailto:bahelms@lbl.gov)

### Authors

**Zhen Xu** — *Materials Sciences Division, Lawrence Berkeley National Laboratory, Berkeley 94720 California, United States*; [orcid.org/0000-0001-9198-3636](https://orcid.org/0000-0001-9198-3636)

**Mason L. Witko** — *Department of Chemistry, University of California, Berkeley 94720 California, United States*

**Hongqian Zheng** — *Department of Materials Sciences and Engineering, University of California Berkeley, Berkeley*

*94720 California, United States*; [orcid.org/0009-0004-3347-8155](https://orcid.org/0009-0004-3347-8155)

**Julia Im** — *Department of Chemical and Biomolecular Engineering, University of California, Berkeley 94720 California, United States*; [orcid.org/0000-0002-6633-2513](https://orcid.org/0000-0002-6633-2513)

**Shira Haber** — *Materials Sciences Division, Lawrence Berkeley National Laboratory, Berkeley 94720 California, United States*; Present Address: Department of Chemistry, Ben-Gurion University of the Negev, Beer-Sheva 84105, Israel; [orcid.org/0009-0003-6916-4871](https://orcid.org/0009-0003-6916-4871)

**Ankita Ghosh** — *Department of Chemistry, University of California, Berkeley 94720 California, United States*

**Maxwell C. Venetos** — *Department of Materials Sciences and Engineering, University of California Berkeley, Berkeley 94720 California, United States*

**Jeffrey A. Reimer** — *Materials Sciences Division, Lawrence Berkeley National Laboratory, Berkeley 94720 California, United States*; *Department of Chemical and Biomolecular Engineering, University of California, Berkeley 94720 California, United States*

**Kristin A. Persson** — *Materials Sciences Division, Lawrence Berkeley National Laboratory, Berkeley 94720 California, United States*; *Department of Materials Sciences and Engineering, University of California Berkeley, Berkeley 94720 California, United States*; *The Molecular Foundry, Lawrence Berkeley National Laboratory, Berkeley 94720 California, United States*; [orcid.org/0000-0003-2495-5509](https://orcid.org/0000-0003-2495-5509)

Complete contact information is available at:

<https://pubs.acs.org/doi/10.1021/jacs.5c06626>

## Notes

The authors declare the following competing financial interest(s): B.A.H., Z.X., M.W., H.Z., M.C.V., and K.A.P. are inventors on the US provisional patent application 63/775,794 (filed 21 March 2025) submitted jointly by Lawrence Berkeley National Laboratory and the University of California, Berkeley that covers cycloolefin resin materials as well as aspects of their use and recovery. B.A.H. has a financial interest in Sepion Technologies and Cyklos Materials. The remaining authors declare no competing interests.

## ACKNOWLEDGMENTS

This material is based upon work supported by the National Science Foundation under Grant 2036849. S.H. and J.A.R. acknowledge support from the U.S. Department of Energy, Office of Science, Office of Basic Energy Sciences, Materials Sciences and Engineering Division for financial support under contract no. DE-AC02-05CH11231, Unlocking Chemical Circularity in Recycling by Controlling Polymer Reactivity across Scales program CUP-LBL-Helms to conduct NMR and mechanical characterization of the thermosets. The solids NMR instrument used in this work is supported by the National Science Foundation under Grant No. 2018784. We thank Drs. Hasan Celik and Raynald Giovine as well as the Pines Magnetic Resonance Center's Core NMR Facility (PMRC Core) for spectroscopic assistance. Work at the Molecular Foundry—including polymer synthesis, deconstruction, and characterization—was supported by the Office of Science, Office of Basic Energy Sciences, of the U.S. Department of Energy under Contract No. DE-AC02-

05CH11231. Computation was carried out at the National Energy Research Scientific Computing Center (NERSC), a U.S. Department of Energy Office of Science User Facility operated under the same contract. We would further like to thank Brian Leal and Raymond Weitekamp of polySpectra for supplying the 3D-printed COR Alpha parts used in this study.

## REFERENCES

- (1) Robertson, I. D.; Yourdkhani, M.; Centellas, P. J.; Aw, J. E.; Ivanoff, D. G.; Goli, E.; Lloyd, E. M.; Dean, L. M.; Sottos, N. R.; Geubelle, P. H.; Moore, J. S.; White, S. R. Rapid Energy-Efficient Manufacturing of Polymers and Composites via Frontal Polymerization. *Nature* **2018**, *557* (7704), 223–227.
- (2) Lee, Y. B.; Suslick, B. A.; de Jong, D.; Wilson, G. O.; Moore, J. S.; Sottos, N. R.; Braun, P. V. A Self-Healing System for Polydicyclopentadiene Thermosets. *Adv. Mater.* **2024**, *36* (11), 2309662.
- (3) McFadden, T. P.; Cope, R. B.; Muhlestein, R.; Layton, D. J.; Lessard, J. J.; Moore, J. S.; Sigman, M. S. Using Data Science Tools to Reveal and Understand Subtle Relationships of Inhibitor Structure in Frontal Ring-Opening Metathesis Polymerization. *J. Am. Chem. Soc.* **2024**, *146* (24), 16375–16380.
- (4) Kovačič, S.; Slugovc, C. Ring-Opening Metathesis Polymerisation Derived Poly(Dicyclopentadiene) Based Materials. *Mater. Chem. Front.* **2020**, *4*, 2235–2255.
- (5) White, S. R.; Sottos, N. R.; Geubelle, P. H.; Moore, J. S.; Kessler, M. R.; Sriram, S. R.; Brown, E. N.; Viswanathan, S. Autonomic Healing of Polymer Composites. *Nature* **2001**, *409* (6822), 794–797.
- (6) Toohey, K. S.; Sottos, N. R.; Lewis, J. A.; Moore, J. S.; White, S. R. Self-Healing Materials with Microvascular Networks. *Nat. Mater.* **2007**, *6* (8), 581–585.
- (7) Cooper, J. C.; Paul, J. E.; Ramlawi, N.; Saengow, C.; Sharma, A.; Suslick, B. A.; Ewoldt, R. H.; Sottos, N. R.; Moore, J. S. Reprocessability in Engineering Thermosets Achieved Through Frontal Ring-Opening Metathesis Polymerization. *Adv. Mater.* **2024**, *36*, 2402627.
- (8) Dean, L. M.; Wu, Q.; Alshangiti, O.; Moore, J. S.; Sottos, N. R. Rapid Synthesis of Elastomers and Thermosets with Tunable Thermomechanical Properties. *ACS Macro Lett.* **2020**, *9* (6), 819–824.
- (9) Sample, C. S.; Hoehn, B. D.; Hillmyer, M. A. Cross-Linked Polyolefins through Tandem ROMP/Hydrogenation. *ACS Macro Lett.* **2024**, *13* (4), 395–400.
- (10) Phatake, R. S.; Masarwa, A.; Lemcoff, N. G.; Reany, O. Tuning Thermal Properties of Cross-Linked DCPD Polymers by Functionalization, Initiator Type and Curing Methods. *Polym. Chem.* **2020**, *11*, 1742–1751.
- (11) Chen, J.; Burns, F. P.; Moffitt, M. G.; Wulff, J. E. Thermally Crosslinked Functionalized Polydicyclopentadiene with a High  $T_g$  and Tunable Surface Energy. *ACS Omega* **2016**, *1* (4), 532–540.
- (12) Leguizamón, S. C.; Cook, A. W.; Appelhans, L. N. Employing Photosensitizers for Rapid Olefin Metathesis Additive Manufacturing of Poly(Dicyclopentadiene). *Chem. Mater.* **2021**, *33* (24), 9677–9689.
- (13) Hausladen, M. M.; Baca, E.; Nogales, K. A.; Appelhans, L. N.; Kaehr, B.; Hamel, C. M.; Leguizamón, S. C. Volumetric Additive Manufacturing of Dicyclopentadiene by Solid-State Photopolymerization. *Adv. Sci.* **2024**, *11*, 2402385.
- (14) Foster, J. C.; Cook, A. W.; Monk, N. T.; Jones, B. H.; Appelhans, L. N.; Redline, E. M.; Leguizamón, S. C. Continuous Additive Manufacturing Using Olefin Metathesis. *Adv. Sci.* **2022**, *9* (14), 2200770.
- (15) Davydovich, O.; Paul, J. E.; Feist, J. D.; Aw, J. E.; Balta Bonner, F. J.; Lessard, J. J.; Tawfick, S.; Xia, Y.; Sottos, N. R.; Moore, J. S. Frontal Polymerization of Dihydrofuran Comonomer Facilitates Thermoset Deconstruction. *Chem. Mater.* **2022**, *34* (19), 8790–8797.
- (16) Sathe, D.; Yoon, S.; Wang, Z.; Chen, H.; Wang, J. Deconstruction of Polymers through Olefin Metathesis. *Chem. Rev.* **2024**, *124* (11), 7007–7044.
- (17) Zheng, K.; Yang, J.; Luo, X.; Xia, Y. High Molecular Weight Semicrystalline Substituted Polycyclohexene From Alternating Copolymerization of Butadiene and Methacrylate and Its Ambient Depolymerization. *J. Am. Chem. Soc.* **2024**, *146*, 25321–25327.
- (18) Ibrahim, T.; Kendzulak, K.; Ritacco, A.; Monetti, M.; Sun, H. Functional Group Transformation Approach to Chemically Recyclable Polymers from Ultra-Low to Moderate Strain Monomers. *Macromolecules* **2025**, *58*, 3898–3905.
- (19) Foster, J. C.; Dishner, I. T.; Damron, J. T.; Kertesz, V.; Popovs, I.; Saito, T. Toward Efficient Entropic Recycling by Mastering Ring-Chain Kinetics. *Macromolecules* **2025**, *58*, 2694–2700.
- (20) Shieh, P.; Zhang, W.; Husted, K. E. L.; Kristufek, S. L.; Xiong, B.; Lundberg, D. J.; Lem, J.; Veyssset, D.; Sun, Y.; Nelson, K. A.; Plata, D. L.; Johnson, J. A. Cleavable Comonomers Enable Degradable, Recyclable Thermoset Plastics. *Nature* **2020**, *583* (7817), 542–547.
- (21) Si, G.; Chen, C. Cyclic–Acyclic Monomers Metathesis Polymerization for the Synthesis of Degradable Thermosets, Thermoplastics and Elastomers. *Nat. Synth.* **2022**, *1* (12), 956–966.
- (22) Huang, B.; Wei, M.; Vargo, E.; Qian, Y.; Xu, T.; Toste, F. D. Backbone-Photodegradable Polymers by Incorporating Acylsilane Monomers via Ring-Opening Metathesis Polymerization. *J. Am. Chem. Soc.* **2021**, *143* (43), 17920–17925.
- (23) Si, G.; Wang, Z.; Zou, C.; Chen, C. Tandem Olefin Metathesis Polymerization to Access Degradable and Recyclable Thermosets, Thermoplastics, and Elastomers. *CCS Chem.* **2025**, *7*, 883–892.
- (24) Lloyd, E. M.; Cooper, J. C.; Shieh, P.; Ivanoff, D. G.; Parikh, N. A.; Mejia, E. B.; Husted, K. E. L.; Costa, L. C.; Sottos, N. R.; Johnson, J. A.; Moore, J. S. Efficient Manufacture, Deconstruction, and Upcycling of High-Performance Thermosets and Composites. *ACS Appl. Eng. Mater.* **2023**, *1*, 477–485.
- (25) Husted, K. E. L.; Shieh, P.; Lundberg, D. J.; Kristufek, S. L.; Johnson, J. A. Molecularly Designed Additives for Chemically Deconstructable Thermosets without Compromised Thermomechanical Properties. *ACS Macro Lett.* **2021**, *10* (7), 805–810.
- (26) AlFaraj, Y. S.; Mohapatra, S.; Shieh, P.; Husted, K. E. L.; Ivanoff, D. G.; Lloyd, E. M.; Cooper, J. C.; Dai, Y.; Singhal, A. P.; Moore, J. S.; Sottos, N. R.; Gomez-Bombarelli, R.; Johnson, J. A. A Model Ensemble Approach Enables Data-Driven Property Prediction for Chemically Deconstructable Thermosets in the Low-Data Regime. *ACS Cent. Sci.* **2023**, *9* (9), 1810–1819.
- (27) Feist, J. D.; Lee, D. C.; Xia, Y. A Versatile Approach for the Synthesis of Degradable Polymers via Controlled Ring-Opening Metathesis Copolymerization. *Nat. Chem.* **2022**, *14* (1), 53–58.
- (28) Christensen, P. R.; Scheuermann, A. M.; Loeffler, K. E.; Helms, B. A. Closed-Loop Recycling of Plastics Enabled by Dynamic Covalent Diketoenamine Bonds. *Nat. Chem.* **2019**, *11* (5), 442–448.
- (29) Lei, Z.; Chen, H.; Luo, C.; Rong, Y.; Hu, Y.; Jin, Y.; Long, R.; Yu, K.; Zhang, W. Recyclable and Malleable Thermosets Enabled by Activating Dormant Dynamic Linkages. *Nat. Chem.* **2022**, *14* (12), 1399–1404.
- (30) Wu, X.; Hartmann, P.; Berne, D.; De bruyn, M.; Cuminet, F.; Wang, Z.; Zechner, J. M.; Boese, A. D.; Placet, V.; Caillol, S.; Barta, K. Closed-Loop Recyclability of a Biomass-Derived Epoxy-Amine Thermoset by Methanolysis. *Science* **2024**, *384* (6692), No. ead9989.
- (31) Demarteau, J.; Cousineau, B.; Wang, Z.; Bose, B.; Cheong, S.; Lan, G.; Baral, N. R.; Teat, S. J.; Scown, C. D.; Keasling, J. D.; Helms, B. A. Biorenewable and Circular Polydiketoenamine Plastics. *Nat. Sustain.* **2023**, *6* (11), 1426–1435.
- (32) Machado, T. O.; Stubbs, C. J.; Chiaradia, V.; Alraddadi, M. A.; Brandolese, A.; Worch, J. C.; Dove, A. P. A Renewably Sourced, Circular Photopolymer Resin for Additive Manufacturing. *Nature* **2024**, *629* (8014), 1069–1074.
- (33) Sathe, D.; Zhou, J.; Chen, H.; Su, H.-W.; Xie, W.; Hsu, T.-G.; Schrage, B. R.; Smith, T.; Ziegler, C. J.; Wang, J. Olefin Metathesis-Based Chemically Recyclable Polymers Enabled by Fused-Ring Monomers. *Nat. Chem.* **2021**, *13* (8), 743–750.



- (34) Xu, Z.; Liang, Y.; Ma, X.; Chen, S.; Yu, C.; Wang, Y.; Zhang, D.; Miao, M. Recyclable Thermoset Hyperbranched Polymers Containing Reversible Hexahydro-s-Triazine. *Nat. Sustain.* **2020**, *3* (1), 29–34.
- (35) García, J. M.; Jones, G. O.; Virwani, K.; McCloskey, B. D.; Boday, D. J.; ter Huurne, G. M.; Horn, H. W.; Coady, D. J.; Bintaleb, A. M.; Alabdulrahman, A. M. S.; Alsewaleim, F.; Almegren, H. A. A.; Hedrick, J. L. Recyclable, Strong Thermosets and Organogels via Paraformaldehyde Condensation with Diamines. *Science* **2014**, *344* (6185), 732–735.
- (36) Pracht, P.; Bohle, F.; Grimme, S. Automated Exploration of the Low-Energy Chemical Space with Fast Quantum Chemical Methods. *Phys. Chem. Chem. Phys.* **2020**, *22* (14), 7169–7192.
- (37) Marenich, A. V.; Cramer, C. J.; Truhlar, D. G. Universal Solvation Model Based on Solute Electron Density and on a Continuum Model of the Solvent Defined by the Bulk Dielectric Constant and Atomic Surface Tensions. *J. Phys. Chem. B* **2009**, *113* (18), 6378–6396.
- (38) Suslick, B. A.; Alzate-Sanchez, D. M.; Moore, J. S. Scalable Frontal Oligomerization: Insights from Advanced Mass Analysis. *Macromolecules* **2022**, *55* (18), 8234–8241.
- (39) Coia, B. M.; Hudson, L. A.; Specht, A. J.; Kennemur, J. G. Substituent Effects on Torsional Strain in Cyclopentene Derivatives: A Computational Study. *J. Phys. Chem. A* **2023**, *127* (23), 5005–5017.
- (40) Vougioukalakis, G. C.; Grubbs, R. H. Ruthenium-Based Heterocyclic Carbene-Coordinated Olefin Metathesis Catalysts. *Chem. Rev.* **2010**, *110* (3), 1746–1787.
- (41) Jacobson, H.; Stockmayer, W. H. Intramolecular Reaction in Polycondensations. I. The Theory of Linear Systems. *J. Chem. Phys.* **1950**, *18* (12), 1600–1606.
- (42) Bates, J. M.; Lummiss, J. A. M.; Bailey, G. A.; Fogg, D. E. Operation of the Boomerang Mechanism in Olefin Metathesis Reactions Promoted by the Second-Generation Hoveyda Catalyst. *ACS Catal.* **2014**, *4* (7), 2387–2394.
- (43) Huang, J.; David, A.; Le Gac, P.-Y.; Lorthioir, C.; Coelho, C.; Richaud, E. Thermal Oxidation of Poly(Dicyclopentadiene)—Kinetic Modeling of Double Bond Consumption. *Polym. Degrad. Stab.* **2019**, *166*, 258–271.
- (44) Davidson, T. A.; Wagener, K. B.; Priddy, D. B. Polymerization of Dicyclopentadiene: A Tale of Two Mechanisms. *Macromolecules* **1996**, *29* (2), 786–788.
- (45) Oromiehie, A.; Mamizadeh, A. Recycling PET Beverage Bottles and Improving Properties. *Polym. Int.* **2004**, *53* (6), 728–732.
- (46) Curtzwiler, G. W.; Schweitzer, M.; Li, Y.; Jiang, S.; Vorst, K. L. Mixed Post-Consumer Recycled Polyolefins as a Property Tuning Material for Virgin Polypropylene. *J. Clean. Prod.* **2019**, *239*, 117978.
- (47) Yang, G.; Mauldin, T. C.; Lee, J. K. Cure Kinetics and Physical Properties of Poly(Dicyclopentadiene/5-Ethylidene-2-Norbornene) Initiated by Different Grubbs' Catalysts. *RSC Adv.* **2015**, *5* (73), 59120–59130.
- (48) Gringolts, M. L.; Denisova, Y. I.; Shandryuk, G. A.; Krentsel, L. B.; Litmanovich, A. D.; Finkelshtein, E. S.; Kudryavtsev, Y. V. Synthesis of Norbornene-Cyclooctene Copolymers by the Cross-Metathesis of Polynorbornene with Polyoctenamer. *RSC Adv.* **2015**, *5* (1), 316–319.
- (49) Walker, R.; Conrad, R. M.; Grubbs, R. H. The Living ROMP of Trans-Cyclooctene. *Macromolecules* **2009**, *42* (3), 599–605.



CAS BIOFINDER DISCOVERY PLATFORM™

## STOP DIGGING THROUGH DATA —START MAKING DISCOVERIES

CAS BioFinder helps you find the  
right biological insights in seconds

Start your search

**CAS**  
A Division of the  
American Chemical Society